World Journal of Surgical Oncology

RESEARCH

Open Access

eIF6: a promising therapeutic target for gastric carcinoma via PI3K/AKT pathway modulation

Shuang Hou[1,2†], Hao Tang[3†], Zhikun Dong[4] and Wence Zhou[1,2*]

Abstract

Background Gastric carcinoma (GC) is a leading cause of cancer-related deaths, with a dire prognosis for advanced stages. The molecular mechanisms underlying GC progression are not fully understood, necessitating research into novel biomarkers and therapeutic targets. This study investigates the role of eukaryotic translation initiation factor 6 (eIF6) in GC, focusing on its potential as a prognostic indicator and its impact on tumor biology.

Methods We analyzed eIF6 expression in GC tissues using data from TCGA and GEO databases. Experiments included western blot, IHC staining, and cell culture assays on GC cell lines to evaluate the effect of eIF6 on cell proliferation, invasion, and apoptosis. Statistical analyses were performed using Student's t-tests and ANOVA, with significance set at $p < 0.05$.

Results eIF6 was found to be significantly overexpressed in GC tissues, associated with advanced tumor stage and poor patient survival. Functional assays demonstrated that eIF6 knockdown inhibits GC cell proliferation and invasion while promoting apoptosis. Transcriptomic analysis linked eIF6 to the PI3K/AKT pathway, a critical regulator in cancer.

Conclusions eIF6's overexpression in GC suggests its role in tumor progression, highlighting its potential as a therapeutic target. The study provides a foundation for developing targeted therapies against eIF6 and emphasizes the need for further research into its regulatory mechanisms in GC.

Keywords Gastric carcinoma, EIF6, Biomarker, Prognosis, PI3K/AKT pathway, Targeted therapy

Background

Globally, gastric cancer (GC) is the fifth most prevalent cancer to be diagnosed and to be fata [1]. The overall 5-year survival rate for people in advanced stages of the disease remains quite low, even with significant advancements in GC diagnosis and treatment. Although there has been some improvement, most patients who get chemotherapy as their first-line neoadjuvant or adjuvant therapy are identified at an advanced stage. Clarifying the distinct biological mechanisms that underlie the beginning and progression of GC is crucial, as is looking into potential targets for early diagnosis and better therapeutic results.

†Shuang Hou and Hao Tang contributed equally to this work.

*Correspondence:
Wence Zhou
zhouwc129@163.com
[1] The Second Hospital & Clinical Medical School, Lanzhou University, Lanzhou, China
[2] Department of General Surgery, The Second Hospital & Clinical Medical School, Lanzhou University, Lanzhou, China
[3] Department of Pharmacy, Songjiang Hospital, Shanghai Jiao Tong University School of Medicine, Shanghai, China
[4] The First Clinical Medical Collegeofaq, Lanzhou University, Lanzhou, China

The fundamental macromolecular machinery that powers protein synthesis in all organisms is the ribosome. The 18S ribosomal RNA [rRNA] is found in the small 40S subunit, while the 28S, 5.8S, and 5S rRNAs are found in the giant 60S subunit, combine to create actively translating 80S ribosomes, the building blocks of eukaryotic ribosomes [2]. It has been established that abnormalities of protein translation and cancer associated pathways contribute to the initiation and growth of tumors and may affect the prognosis of cancer patients [3, 4]. Consequently, the dysregulation of translation initiation has received a lot of attention, and several investigations have shown that different cancer entities express abnormal levels of eukaryotic translation initiation factors (eIFs). Patients with lung cancer (LC) or prostate cancer (PCa) often have overexpressed eIF4E [5, 6], The advanced stage of ovarian cancer (OV) is clearly linked to eIF5A2 overexpression, which promotes the epithelial to mesenchymal transition [7]; in breast cancer (BC), eIF3D mediates selective mRNA translation, which promotes the cell mesenchymal transition and metastasis [8].

Eukaryotic translation initiation factor 6 (eIF6) is known as a 27 kDa protein that has been conserved throughout evolution. It controls the interaction of 40S and 60S ribosomal subunits, which is important for ribosomal biogenesis and translation regulation. eIF6 has been demonstrated to have two distinct functions in the past: In both yeast and mammals, nucleolar eIF6 is required for the synthesis of 60S subunits, while in mammals, cytoplasmic eIF6 is required for translation that is accelerated by growth hormones and insulin. These studies demonstrated the significance of eIF6 in carcinogenesis, cell cycle progression, and cancer cells invasiveness [4, 9, 10] dysregulation of eIF6 is a crucial regulator in the development of esophageal, breast, and liver hepatocellular carcinomas, respectively [11–13].

Our goal in this work was to examine eIF6's possible function and mechanism in the development and spread of GC tumors. Our initial findings, using both the TCGA and GEO databases, showed that eIF6 was significantly overexpressed in GC samples relative to non-neoplastic tissue. This finding was then confirmed by IHC and western blot. Based on the analysis of clinicopathological criteria, we also found a strong correlation between elevated levels of eIF6 and tumor growth. This suggests that eIF6 could be a useful biomarker for both prognosis and diagnosis in patients with GC. Functional research also revealed that eIF6 was a potential driver of tumor biological events in both in vitro along with in vivo tumor settings. Additionally, we used transcriptomics sequencing for signaling pathway enrichment assessment and western blot testing to confirm that eIF6 could trigger PI3K/Akt-related cancer signaling pathways. As a result, our research may offer a novel therapeutic approach for GC that targets eIF6 in GC and has a solid theoretical foundation.

Materials and methods

Bioinformatic analysis

The Cancer Genome Atlas (TCGA) database (https://www.cancer.gov/tcga) provided expression data for 375 STAD samples and 32 adjacent normal tissues. The Gene Expression Omnibus database (GEO, https://www.ncbi.nlm.nih.gov/geo/) provided the five eIF6 expression profiles (GSE66229, GSE29272, GSE26899, GSE13911, and GSE184336). High-throughput sequencing (HTSeq) data from TCGA and GTEx is compiled in the UCSC dataset and is utilized for single-gene pan-cancer research. R software was used to examine all bioinformatics data. Patients with GC were analyzed for overall survival (OS) and disease-specific survival (DSS) using the Kaplan–Meier Plotter website (http://kmplot.com/analysis/).

Tissue specimens and ethics statement

Between 2015 and 2016, patients at The First Hospital of Lanzhou Univers who had surgical resection but did not receive preoperative chemotherapy or radiotherapy provided a total of 100 paraffin-embedded stomach cancer specimens. Eight new main GC parts and the corresponding normal gastric components were immediately stored at −80 °C in the Department of Surgical of our hospital after harsh excision. Table 2 lists the clinicopathological characteristics of the GC patients. This research was approved by the appropriate ethical committee and was carried out in accordance with the Declaration of Helsinki. Each patient provided informed, written consent.

Cell culture and transfection

The GES-1 human gastric epithelial cell line and the GC cells (AGS, KATOIII, HGC-27, HGC-28, MKN-74, and MKN-45) were acquired from the Shanghai Institute of Cell Biology, China Academy of Sciences. RPMI-1640 media or DMEM (Gibco, USA) supplemented with 10% fetal bovine serum (FBS; ABW, Uruguay) were used to maintain the GC cells at 37 °C in a 5% CO2 atmosphere. The appropriate control lentivirus and eIF6 shRNA lentivirus were created and acquired by GenePharma (Shanghai, China). The day before transfection, GC cells were equally plated, As directed by the manufacturer, lentivirus production was performed in infected GC cells, and puromycin (2 μg/ml) was employed to generate stable cell lines.

Western blotting

Using a cocktail of protease and phosphatase inhibitors (KeyGEN, China) and RIPA buffer (Beyotime, China), From cells or tissues, total proteins were isolated. The level of protein was determined using a BCA Protein Assay kit (Solarbio, China). Proteins isolated by 10% SDS-PAGE were then transferred onto polyvinylidene difluoride (PVDF) membranes (Millipore, USA). PVDF membranes were blocked with a solution of 5% nonfat milk in 1% Tween-PBS (TBST) for at least an hour at room temperature. The membranes were then treated with the specified primary antibodies (Table 1) for an entire night at 4 degrees Celsius. After three separate 10-min TBST washes, membranes were then incubated for one hour at room temperature with matched second antibodies (Table 1). The Pierce ECL Western Blotting Substrate (Beyotime, China) and chemiluminescence imaging system (Tanon, China) were utilized to probe the blots. β-actin served as the internal control when quantifying the protein bands' gray values using ImageJ software.

Table 1 Correlation between eIF6 expression and clinicopathological characters of patients with gastric cancer (IHC)

Characteristics	Low	High	P value
n	37	63	
Sex, n (%)			0.644
Male	28 (28%)	45 (45%)	
Female	9 (9%)	18 (18%)	
Age (yr), n (%)			0.907
< 60	21 (21%)	35 (35%)	
≥ 60	16 (16%)	28 (28%)	
Histologic type, n (%)			0.983
Undifferentiated	24 (24%)	41 (41%)	
Differentiated	13 (13%)	22 (22%)	
Pathologic T-category, n (%)			0.457
T1-2	7 (7%)	16 (16%)	
T3-4	30 (30%)	47 (47%)	
pTNM stage, n (%)			0.014
I-II	21 (21%)	20 (20%)	
III-IV	16 (16%)	43 (43%)	
Tumor size (cm), n (%)			0.219
≤ 3	15 (15%)	18 (18%)	
> 3	22 (22%)	45 (45%)	
Tumor location, n (%)			0.155
Lower/Middle	29 (29%)	56 (56%)	
Upper	8 (8%)	7 (7%)	
Lymphatic invasion, n (%)			0.564
Positive	16 (16%)	31 (31%)	
Negative	21 (21%)	32 (32%)	

Immunohistochemistry (IHC) staining

The process of staining using immunohistochemistry (IHC) was developed using earlier techniques that were documented in the literature. The application of eIF6 and Ki67-specific antibodies (Table 1) followed the manufacturer's instructions. The staining intensity multiplied by the percentage of positively stained cells yields the score index (SI) scores, which are used by two pathologists to blindly evaluate the IHC data. The percentage was assessed as 0 (0%), 1 (0–25%), 2 (25–50%), 3 (50–75%), and 4 (75–100%), whilst the degree of staining was graded as 0 (negative), 1 (weak), 2 (moderate), and 3 (strong). Samples with a SI score below six were considered as having weak eIF6 expression, whereas samples with a score of six or more were considered to have strong eIF6 expression.

Assays for colony formation and cell proliferation

Using the Cell Counting Kit-8 (CCK-8) (Beyotime, China), the rate of cell proliferation was determined. In 96-well plates, control and transfected GC cells were planted at similar densities (1000 cells/well) and grown at 37 °C with 5% CO2. Then, at0,1,2, and 3 days after plating, 10 μl of CCK-8 reagent was applied to each well. After two more hours of incubation at 37 °C, the optical density (OD) of the plate was determined using automatic enzyme labeling (Molecular Devices, Sunnyvale, CA) at 450 nm. Every sample was triplicated and independently replicated three times. Cells were seeded at the appropriate cell number into 12-well plates for the EdU test. The cells were co-cultured with EdU working solution for two hours on the next day. Following the directions provided by EdU (from Beyotime, China), fixation and staining were carried out, and fluorescence microscope photos were taken.

Transfected GC cells were plated into 6-well plates in equal quantities (0.8 × 103/well), and the media was changed every two days until the colonies became visible to the unaided eye after about two weeks. Following that, the cells were fixed for 20 min at room temperature using 4% paraformaldehyde (PFA) and 0.1% crystal violet dye. ImageJ was used to count the colonies. Every biological experiment was carried out a minimum of three times.

Cell cycle and apoptosis analysis

Six-well plates were used to plate GC cells transfected with lentiviral suppressing eIF6 along with the control group. Trypsin without EDTA was used to break down the cells once confluence reached 70–80%, and the cells were then gathered in binding buffer. As directed by the manufacturer, the tests for the cell cycle and apoptosis were carried out using the Cell Cycle Detection

Kit (KeyGEN, China) and the Annexin V-APC/7-AAD Apoptosis Detection Kit (KeyGEN, China), respectively. A BD FACSCanto II flow cytometer (BD Biosciences) with ModFit LT software (Verity Software House, Topsham, ME) was used to evaluate the flow cytometry result. Every test was conducted three times.

Assays for cell transwell Matrigel invasion

The 24-well plates were lined with eight-micrometer-pore-sized special chambers (Corning, USA) and covered with 50 µl of diluted Matrigel (1:5 in RPMI 1640 medium; ABW, USA) for a duration of four hours. The bottom chambers held 600 µL of 1640 media supplemented with 20% FBS, while the upper chamber held treated cells (1×105/well) suspended in 200 µL serum-free medium. The cells that invaded the transwell chambers' underside were grown in a thermostatic incubator for a whole day at 37 °C. After that, they were dyed with 0.1% crystal violet for 20 min at room temperature and fixed for 30 min with 4% paraformaldehyde. The number of invasive cells was measured under a microscope in five distinct visual regions (Olympus, Japan).

Cell transwell assay

Cells without FBS were cultivated in Transwell plate top chamber cultures. To the lower chamber, 600 ul of complete culture media containing 20% FBS was introduced. After a 24-h incubation period, the cells on the upper side of the basal membrane were removed using a sterile cotton swab. The cells were fixed with 4% paraformaldehyde and then dyed with 1% crystal violet. The invader cells were counted under a microscope (Olympus, Japan).

Transcriptomics

Liquid nitrogen was used to harvest the stably transfected stomach cells ($n=3$ for each group) of sh-CON and sh#1. Using Trizol reagent (Invitrogen, Carlsbad, CA, USA), following the manufacturer's guidelines, total RNA was extracted and purified. An instrument called the NanoDrop ND-1000 (NanoDrop, Wilmington, DE, USA) was used to calculate the amount of RNA in each sample. Ultimately, we employed an Illumina NovaSeqTM 6000 (LC-Bio Technology Co., Ltd., Hangzhou, China) for 2×150 bp paired-end sequencing (PE150), adhering to the vendor's suggested technique. The nested linear models (p value <0.05) were compared using the R package edgeR and a parametric F-test. mRNAs that expressed differently were selected based on a fold change of >2 or <0.5. RNA sequencing and bioinformatics analysis were outsourced to LC-BIO TECHNOLOGIES (HANGZHOU, CHINA) CO., LTD.

Subcutaneous xenograft experiment

Four to five week old female BALB/c-nu (nude) mice were housed at the SPF Animal Laboratory. The mice were obtained from the Animal Center of Sichuan Province (Chengdu, China). Stable transfected HGC27 and MKN45 cells (1×107 in 100 µL PBS per mouse) with either control lentiviruses (ShNC) or eIF6 silenced lentiviruses (SheIF6) were injected subcutaneously into the tissues of nude mice. The tumor's size was measured with vernier calipers, and its volume was calculated using the formula $V=1/2\times\text{length}\times\text{width}\times\text{height}$. Four weeks later, mice were sedated while still in their undergarments, and tumors were meticulously removed, weighed, and overnight stored in 10% neutral-buffered formalin. Standard protocols were followed to apply hematoxylin–eosin (HE) and immunohistochemical staining with anti-Ki67 to the generated 4-µm slices. The Second Hospital of Lanzhou University's Animal Care and Use Committee authorized the protocols used in all animal studies.

Statistical analysis

Every study was evaluated using SPSS 22.0, a statistical analysis program. The quantitative results of three independent studies are displayed as means ± standard (means ± SD). One-way ANOVA or a two-tailed Student's t-test were used to compare the groups. Chi-square ($\chi2$) testing were used to investigate the relationships between eIF6 expression and clinicopathologic characteristics. The analysis of survival was done using the Kaplan–Meier method. Using Spearman's correlation coefficient, the linear connection between eIF6 and target genes in GC tissues was examined. When $p<0.05$, it was deemed statistically significant.

Results

eIF6 is overexpressed in GC patient and is related with poor prognosis

The TCGA database was utilized to analyze the eIF6 mRNA expression profiles in pan cancers. The results showed that the expression of eIF6 mRNA was significantly higher in several cancer types, such as ACC, BRCA, BRCA, CESC,CHOL,COAD,DLBC,ESCA, GBM, KIRC, KIRP, LGG, LIHC, LUAD, LUSC,OV, PAAD, PRAD,READ, SKCM, STAD,TGCT,THCA,THYM,UCEC, and UCS, but significantly lower in KICH and PCPG. There was no discernible difference in the expression of the remaining malignancy. Consequently, we assessed the eIF6 levels in the TCGA-STAD datasets. The results showed that eIF6 mRNA expression was significantly elevated in GC (Fig. 1a-b, $P<0.01$). Additionally, using the analysis of the GEO datasets GSE66229, GSE29272,

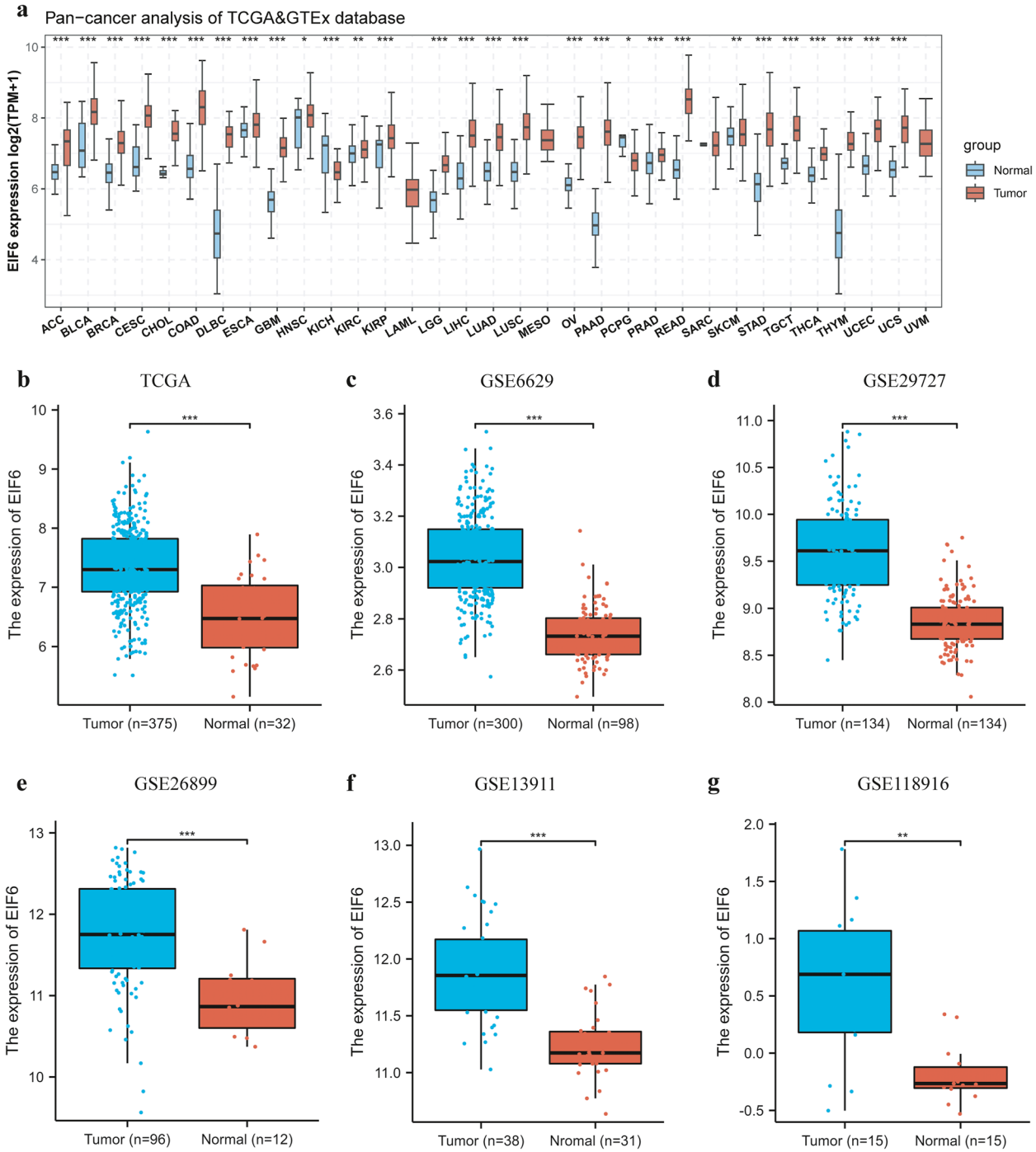

Fig. 1 Bioinformatics study of GC tissues revealed an upregulation of eIF6. **a** The pan-cancer express level of eIF6. **b** According to the TCGA database, GC tissues ($n = 375$) had a higher level of eIF6 expression than regular tissues ($n = 32$). **c**-**g** According to the GEO database, GC tissues had higher levels of eIF6 expression than normal tissues, including GSE66229 (Normal = 98, Tumor = 300), GSE29272 (Normal = 134, Tumor = 134), GSE26899 (Normal = 12, Tumor = 96), GSE13911 (Normal = 31 and Tumor = 38), and GSE118916 (Normal = 15 and Tumor = 15). ***$p < 0.001$. GC is for gastric cancer; TCGA stands for The Cancer Genome Atlas; GEO stands for Gene Expression Omnibus. eIF6, eukaryotic translation initiation factor 6

GSE26899, GSE13911, and GSE118916, we corroborated the high expression of eIF6 in tumor tissues. It was also established that eIF6 was up-regulated in GC (Fig. 1c-j, $P < 0.01$). Using Western blot and IHC labeling, the expression of eIF6 in GC cells and tissues was further confirmed in relation to their matching. as seen in Fig. 2.a-c.

eIF6 expression is positively correlated with pTNM stage and poor prognosis in GC patients

We examined the connection between the expression of eIF6 and the clinical traits of GC patients derived from IHC data in order to learn more about the function of eIF6 in the development of GC. Following their division into two groups ($n = 63$ and $n = 37$), the 100 GC patients were categorized according to their eIF6 expression

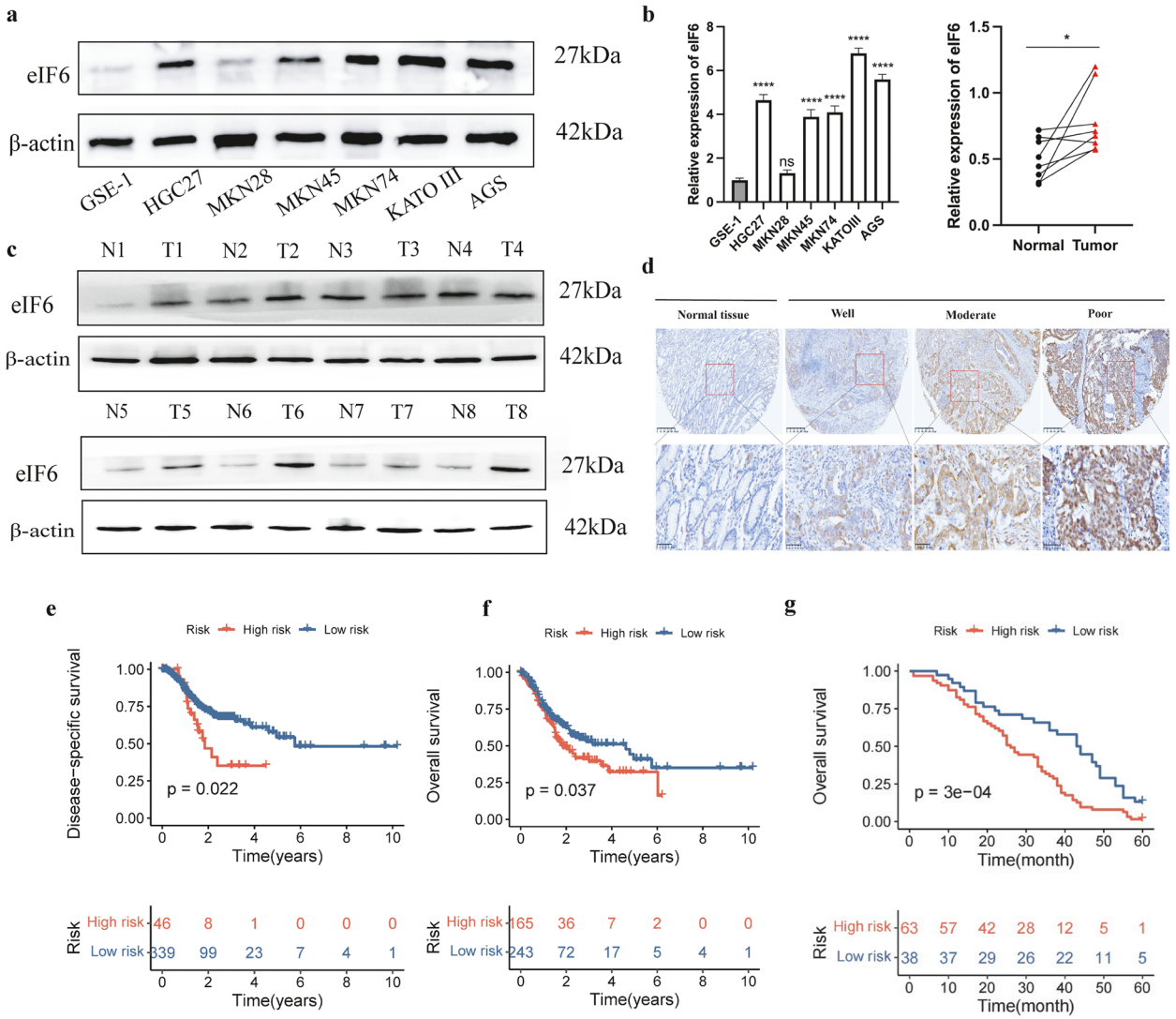

Fig. 2 Poor prognosis and GC advancement are associated with upregulation of eIF6. **a** Western blot was used to measure the eIF6 protein levels in seven GC cell lines. **b** The eIF6 protein level means ± SD ($n = 3$) is displayed. **c** Utilizing Western blot analysis, the levels of eIF6 protein expression were measured in eight pairs of recently surgically removed human GC tissues. An internal control was employed, namely β-actin. The eIF6/β-actin density was calculated based on the relative expression levels of the eIF6 protein. N denotes the adjacent normal stomach tissues; T is the GC tissues. **d** eIF6 antibody IHC staining of GC and normal liver tissues. The eIF6 photos with low expression, moderate expression, and high expression were displayed above. Bar is equal to 50 μm. **e** DSS Kaplan–Meier analysis, Individuals with low eIF6 expression ($n = 339$) f experienced a more depressing DSS than those with high eIF6 expression ($n = 46$). The Kaplan–Meier analysis of OS showed that in GC, the group that had low eIF6 expression ($n = 244$) was higher than the group with high eIF6 expression ($n = 165$).Compared to low eIF6 expression ($n = 38$), our cohort witnessed eIF6 overexpression ($n = 63$) had a poorer survival rate. The mean ± SD ($n = 3$) is represented by the error bar. OS stands for overall survival; DSS for disease-specific survival. $^{**}p < 0.01$; $^{***}p < 0.001$; and $^{*}p < 0.05$

levels. Table 2 provides an overview of these groups' clinical characteristics. The information demonstrates a substantial correlation between the pTNM stage and eIF6 expression. Other clinicopathological characteristics, including as sex, age, tumor size, differentiation, lymphatic metastasis, histologic type, and tumor site, were unrelated to eIF6 overexpression. The eIF6 high expression group's disease-specific survival (DSS) and overall survival (OS) time were found to be significantly shorter in the Kaplan–Meier survival curves compared to the eIF6-low expression group ($p=0.0222$, $p=0.037$) (Fig. 2e,f). Our cohort also confirmed the results (Fig. 2g). These findings suggest a correlation between eIF6 expression and pTNM stage and a bad outcome in patients with HCC.

Knockdown of eIF6 inhibits the malignant progression of GC cells in vitro

In order to confirm the potential biological function of eIF6 in GC cells, we generated stable cell lines, HGC-27 and MKN-45, that had eIF6 knockdown. Western blotting was used to determine the infection efficiency ($p<0.001$) (Fig. 3a). CCK-8 assay results showed that eIF6 knockdown cells' proliferative activity was significantly lower than that of control cells (Fig. 3c,d). According to the quantitative analysis of plate colony assays, there were significantly less colonies formed by eIF6 knockdown cells than by control cells ($p<0.05$) (Fig. 3e). Next, in order to investigate the impact of eIF6 knockdown on tumor migration and invasion in vitro, we performed Transwell and Transwell-Matrigel tests. GC cells' in vitro motility and invasion capacity was significantly reduced ($p<0.001$) by eIF6 knockdown, as seen by the number of cell invasions in the control, sh#1, and sh#2 groups. (Fig. 3f).The results of the Edu tests showed that eIF6 downregulation significantly affects cell proliferation ($p<0.001$) (Fig. 3 g).

Using a western blot and flow cytometry experiment, we were also able to identify the impact of eIF6 on apoptosis and the cell cycle in HGC-27 and MKN-45 cells. Similar to the findings of the proliferation assay, knockdown of eIF6 increased the fraction of HGC-27 and MKN-45 cells in the G0/G1 phase (Fig. 4b). When it came to cell apoptosis, eIF6 knockdown significantly increased the overall apoptosis rate in MKN45 cells ($p<0.01$) and HGC27 cells ($p<0.01$) (Fig. 4a). Thus, our findings suggested that the increase in apoptosis and cell cycle G0/G1-phase arrest may be involved in the inhibition of cell growth following eIF6 depletion. WB also confirmed results that were similar. The results above all implied that eIF6 might encourage the proliferation and invasion of GC cells in vitro.

Knockdown of eIF6 arrested tumor growth in a nude subcutaneous xenograft model

In a nude mouse xenograft model, the impact of eIF6 on GC cell proliferation was further validated. Tumor size was assessed four days after injection of cells treated with eIF6 control (NC) or knockdown (Sh) into nude subcutaneous tissue, respectively. In comparison to the controls, cells injected into the Sh groups formed slower growing tumors ($p<0.05$) and smaller, lighter tumors ($p<0.01$) (Fig. 5a-b). Lastly, HE using Ki-67 antibody IHC staining revealed that the Sh groups had lower levels than the control groups ($p<0.05$) (Fig. 5d–e), further supporting

Table 2 Antibody

Antibody	Company	Catalog#	Size(kDa)	species
eIF6(D16E9)	Cell signaling Technology	3833 T	37 kDa	Rabbit
Phospho-Akt(ser473) (D9E)	Cell signaling Technology	4060 T	60 kDa	Rabbit
Akt(pan)(C67E7)	Cell signaling Technology	4691 T	60 kDa	Rabbit
Phospho-PI3Kinase p85(Tyr458)/p55(Tyr199)	Cell signaling Technology	4228 T	85 kDa	Rabbit
PI3Kinase p85(19H8)	Cell signaling Technology	4257 T	85 kDa	Rabbit
Ki67	Abmart	TW0001	358 kDa	Rabbit
CDK2	Boster	PB9534	30 kDa	Rabbit
Cyclin A (B-8)	Santa cruz	Sc-271682	54 kDa	Mouse
Parp	Abmart	T40050F	89 kDa	Rabbit
Caspase3	Abmart	T40044F	32 kDa	Rabbit
Bcl-2	Abmart	T40056F	26 kDa	Rabbit
Cytochrome C	Abmart	T55734F	15 kDa	Rabbit
B-actin	Servicebio	GB15001-100	42–45 kDa	Mouse
HRP-labeled goat anti-rabbit IgG	Servicebio	GB23303		
HRP-labeled goat anti-mouse IgG	Servicebio	GB23301		

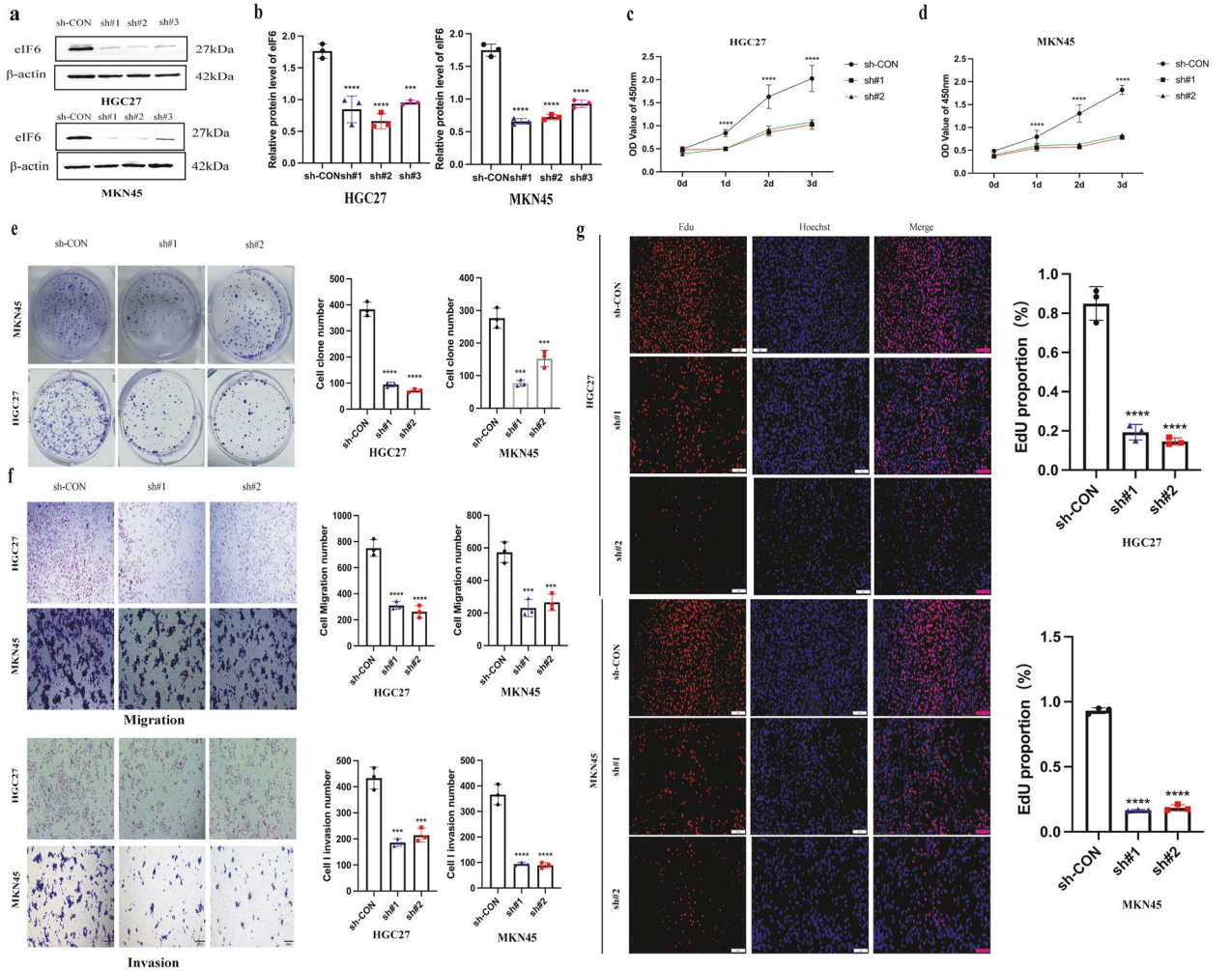

Fig. 3 In vitro GC cell invasion and proliferation were suppressed by eIF6 knockdown. **a** The effectiveness of GC cell-based eIF6 lentivirus knockdown was determined by Western blot analysis. **b** Using the ImageJ program, the Western Blotting's blot density was measured. Loading control was established using β-actin. **c**, **d** The ability of knockdown eIF6 lentivirus-infected HGC27 and MKN45 cells to proliferate was assessed using CCK-8 assays. NC cells and Sh-eIF6 cells in ePlate colony formation experiments (left). After 14 days, The quantity of colonies established was tallied. (right). **f** Transwell invasion tests using matrigel and non-matrix migration assays using Sh-NC and Sh-eIF6 cells (left). In five randomly chosen microscopic fields, the quantity of cells that moved after 24 h was tallied (right). **g** Utilizing the Edu cell proliferation test measure cell proliferation. The signal's quantification was displayed on the right. Bar is equal to 200 μm. The mean ± SD ($n = 3$) is represented by the error bar. $^{**}p < 0.01$; $^{***}p < 0.001$; and $^{*}p < 0.05$

the idea that eIF6 knockdown hindered the proliferation of GC cells in vivo.

Identify the molecular mechanisms and signaling pathways regulated by eIF6

We conducted transcriptome research on HTR-8/SVneo cells in the control and eIF6-knockdown groups in order to better explore the putative signaling pathways through which eIF6 increased tumor malignant development. Comparing the gastric cancer cells with eIF6 knockdown to the control group, transcripts for 1719 DEGs in total were found. Figure 1a shows that 805 of these DEGs were upregulated and 914 were downregulated. The primary enriched GO terms were extracellular matrix architecture, cell adhesion, collagen-containing extracellular matrix, plasma membrane, and extracellular region (Fig. 6b). Representative DEGs were aggregated using a hierarchical clustering technique (Fig. 6c). Upon examining noteworthy pathways discovered using KEGG enrichment (Fig. 6d), we noticed several DEGs connected to the PI3K/AKT signaling pathway, which is linked to the malignant growth of tumor cells.

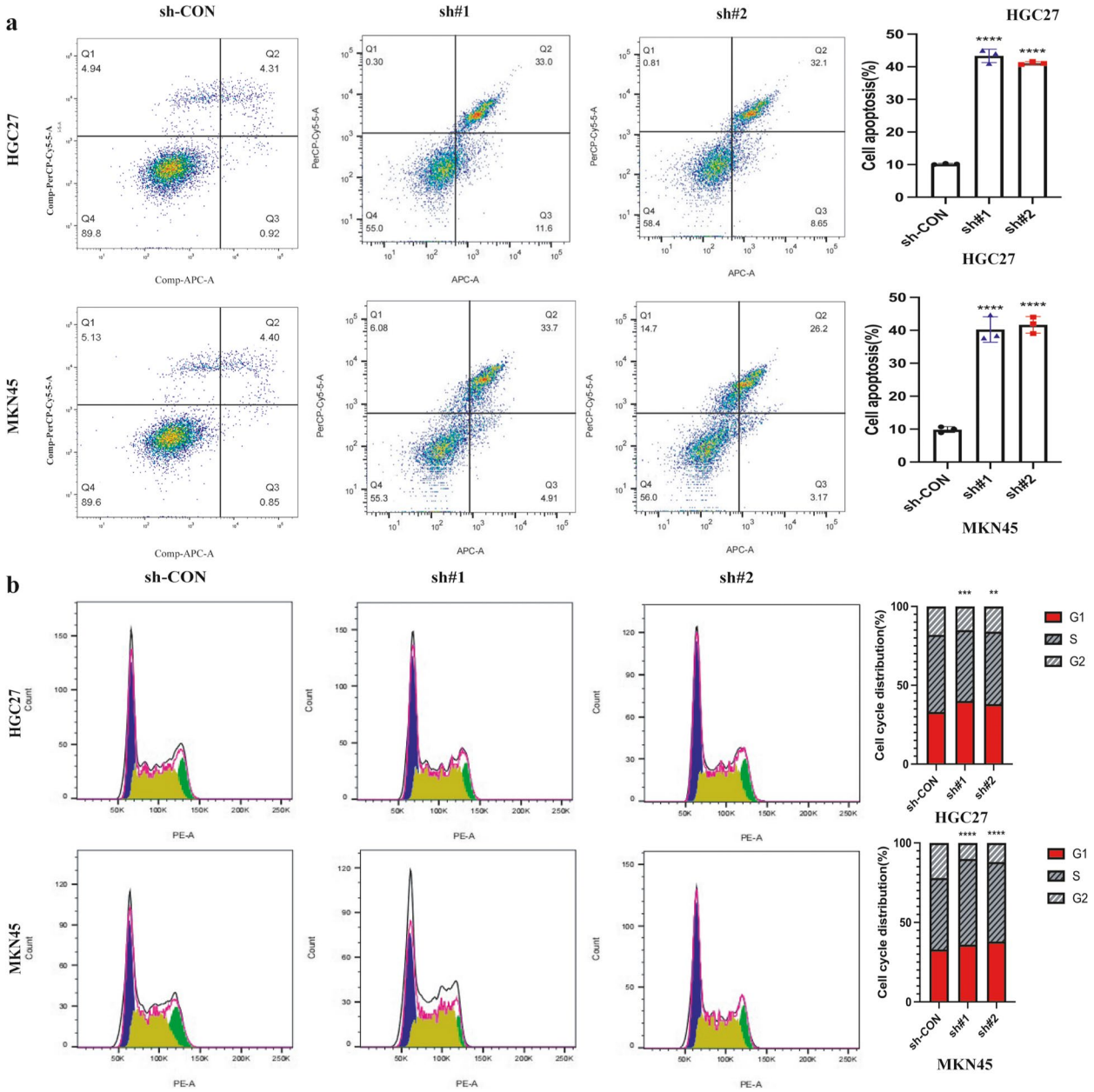

Fig. 4 Apoptosis and cell cycle arrest are caused by eIF6 knockdown. **a** Using flow cytometry, a test for cell apoptosis was carried out (left). Three separate experiments were used to calculate the cell apoptosis rate (right). **b** Using flow cytometry, NC cells and Sh-eIF6 cells underwent a cell cycle experiment (left). Three separate experiments' worth of data on cell cycle distribution were evaluated (right). The mean ± SD ($n = 3$) is represented by the error bar. ****$p < 0.001$; **$p < 0.01$

eIF6 activated PI3K/AKT-related cancer signaling pathways in GC progression

In order to validate the results of the enrichment analysis, we used western blotting to investigate the impact of eIF6 knockdown on PI3K/AKT activity. In the HGC27 and MKN45 cell lines, as demonstrated in Fig. 7e, eIF6 knockdown reduced the level of phosphorylated-PI3K/AKT (p-PI3K/AKT), suggesting an upstream regulatory role for eIF6 on p-PI3K/AKT. Simultaneously, eIF6 knockdown increased the expression of cell cycle regulators such as cyclin A and CDK2, and decreased the expression of Bcl-2, apoptotic regulators Caspase3, cytochrome C, and PARP (Fig. 7a-c). Consistent with the western blot results, eIF6

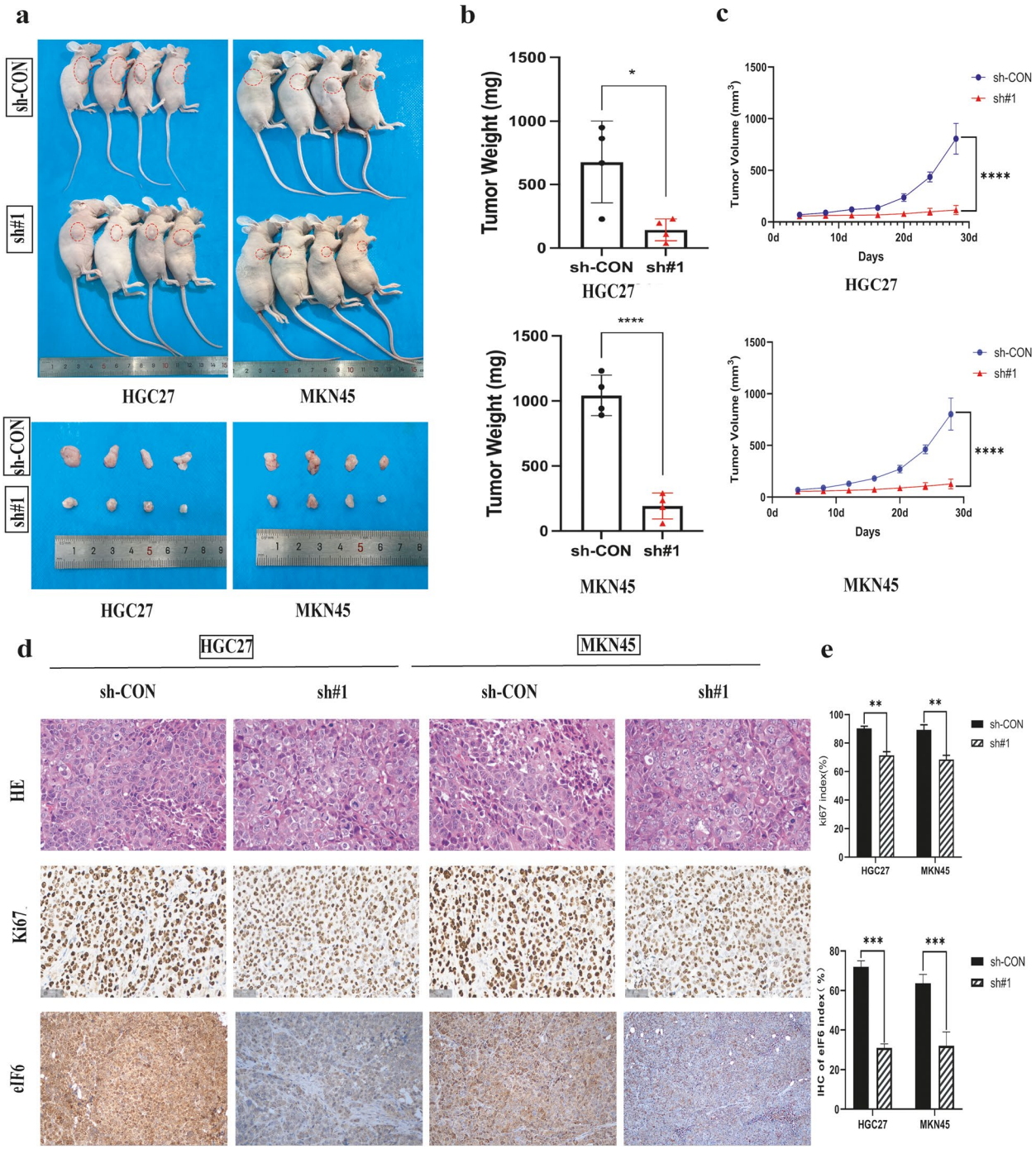

Fig. 5 The ability of GC cells to form tumors in vivo was decreased by eIF6 knockdown. **a** photos of tumors grown in BALB/c nude mice that received subcutaneous injections of MKN45 and eIF6-knockdown HGC27 cells (left, $n = 4$ per group) and each other. **b** When the tumors were perfectly removed from the nude mice, their weights were measured. **c** The days listed were used to compute the tumor volumes. **d** sectioning subcutaneous tumors using HE and IHC and stained with the Ki-67 antibody. Bar is equal to 50 μm. **e** The Ki-67 score was calculated by dividing the overall amount of cells (× 100%) by the quantity of cells expressing Ki-67. The mean ± SD is shown by the error bar. $^{**}p < 0.01$; $^{*}p < 0.05$

expression was connected with cell cycle G1 arrest and call apoptosis, as demonstrated by the identification of a coefficient connection between eIF6 and the aforementioned relevant markers.

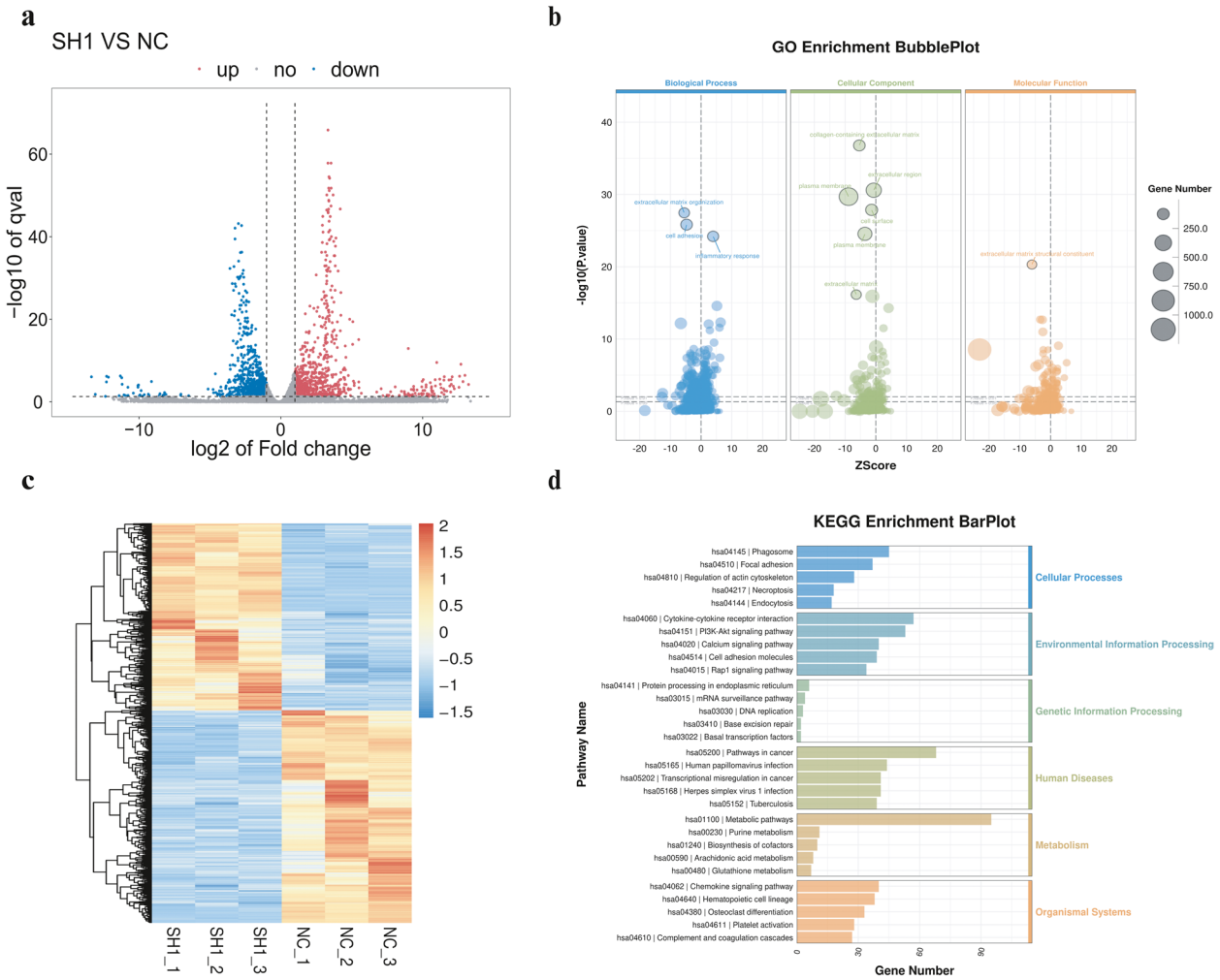

Fig. 6 RNA-seq data for eIF6 knockdown and controls. **a** the DEGs in a volcano layout. Light blue and light red were used to indicate up- and down-regulated DEGs with $p < 0.01$ and a fold change > 2, respectively. **b** Functional classification of the DEGs using Gene Ontology (GO). **c** The DEGs' hierarchical grouping between HCs and PE patients. **d** The functional classification of the DEGs according to the Kyoto Encyclopedia of Genes and Genomes

Discussion

Gastritis is one of the most common malignancies, and it poses a global health risk due to its high fatality rate. New molecular mechanisms underlying its pathogenesis must be identified immediately. The most recent Global Cancer Statistics 2022 report shows that there were about 122,400 deaths and over 122,500 new cases in 2022, placing the disease fifth globally in terms of incidence and mortality. The five years relative survival rate is still a pitiful [1]. Despite advancements in diagnostic techniques and treatment strategies, the prognosis and effectiveness of treatment for stomach cancer remain unsatisfactory. Finding promising molecular treatment targets and applying them to the clinical prognosis of gastric cancer has become one of the major research hotspots.

In eukaryotic cells, translation initiation factors (EIFs) are essential for the phase of protein synthesis that determines rate. They are important for cellular transformation, apoptosis, proliferation and tumorigenesis [14]. The development of cancer, metastasis, and tumor angiogenesis are all impacted by dysregulation of eIFs, which can take the form of over-, down-, or phosphorylation [15]. Indeed, pertinent researches have identified that overexpression of eIFs plays a significant role in the carcinogenesis of a wide range of illnesses. For example, people with lung cancer (LC) or prostate cancer (PCa) often have overexpression of eIF4E [5, 6]. eIF3D mediates selective mRNA translation promotes cell mesenchymal transition and metastasis in Breast cancer (BC) [8], and eIF5A2 overexpression promotes epithelial to mesenchymal

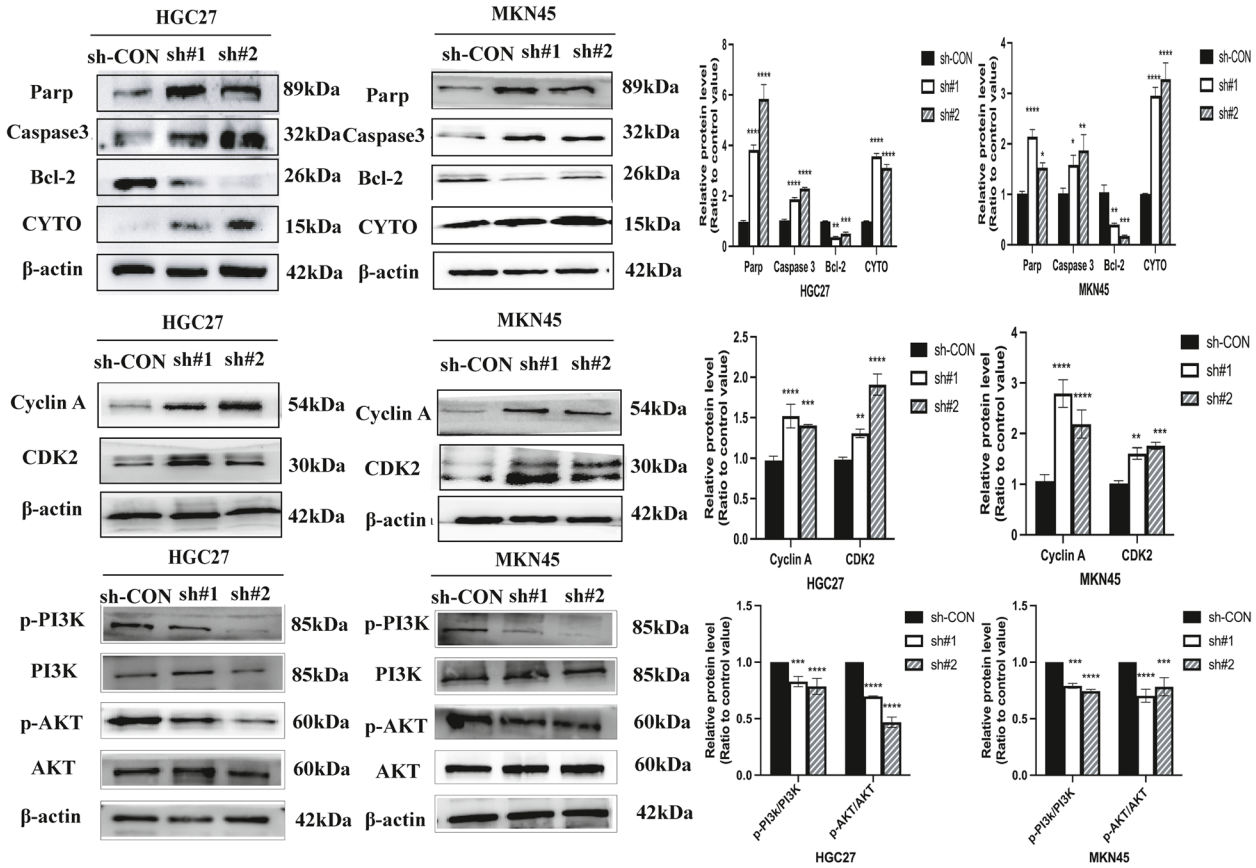

Fig. 7 eIF6 triggered cancer signaling pathways linked to PI3K/AKT in the advancement of GC. **a**,**c** The expression levels of apoptosis and cell cycle markers, such as Parp, Caspase 3, Bcl-2, Cytochrome C, Cyclin A, and CDK2, were measured by western blotting. Using the ImageJ program, the Western Blotting's blot density was measured. Loading control was established using β-actin. **e** Through western blotting, the expression level of markers associated to PI3K/AKT was ascertained. Using the ImageJ program, the Western Blotting's blot density in HGC27 and MKN45 cells (**b**,**d**,**f**) was measured. $^{**}p < 0.01$;$^{***}p < 0.001$; and $^{*}p < 0.05$

transition is clearly connected with the advanced stage of ovarian cancer (OV) [7]. The critical roles that eIFs play in the mechanisms underlying the genesis and evolution of GC, however, are yet unknown.

According to reports, eIF6 is a crucial regulator in the cases of esophageal, breast, and liver hepatocellular carcinomas, respectively [11–13]. Emerging research in recent years has revealed that the protein eIF6 regulates growth factor-induced cancers and the course of tumors [16]. As an anti-association component, it prevents the cytoplasmic assembly of the 60S and 40S ribosomal subunits, eIF6 also plays a function in facilitating the synthesis of 60S ribosomes in the nucleolus16 by being a part of preribosomal particles [17]. Research has shown that the G1/S block caused by eIF6 downregulation can result in aberrant embryonic development [18], and that Saccharomyces cerevisiae cell viability and proliferation are decreased when eIF6 is knocked down [19]. Furthermore, cytoplasmic eIF6 impairment inhabits tumor progression while leaving normal growth unaffected [20]. These studies highlight the critical function that eIF6 plays throughout the cell cycle and the growth of malignancies.

In this work, we first demonstrated that eIF6 was overexpressed in GC and suggested that it could be a useful biomarker in GC patients. The overexpression of eIF6 was found to decrease patients' overall survival in GC, according to our TCGA and GEO data set. This strongly suggests that eIF6 was a predictor of overall survival in GC. Therefore, measuring eIF6 in terms of RNA or protein may help anticipate the emergence of GC, and using genetic interference to specifically target eIF6 may increase the effectiveness of treatment. To further verify eIF6 as a novel prospective target for GC, we performed knockdown studies to investigate the biologic importance of eIF6 in vivo and in vitro tumor models. Following the effective suppression of eIF6, GC cells' capacity for invasion, carcinogenesis, and cell growth rate were all markedly reduced. This is in line with other research that found that eIF6 overexpression in ovarian cancer boosted the migratory phenotype by increasing CDC42

translation, However, CRC cells' eIF6 knockdown significantly decreased their ability to proliferate and colonize [21]. Tumor occurrence is linked to aberrant cell differentiation and proliferation as well as aberrant apoptosis. Tumor regression may thus have a therapeutic effect in conjunction with the spontaneous death of malignant tumors [22]. We also examined the degrees of apoptosis in our investigation, and discovered that eIF6 knockdown considerably raised the apoptosis ratio in transfected GC cells. The activation of cell degeneration pathways is not facilitated by eIF6 silencing in NSCLC cells, since it also elevates p21 and SA-β-Gal activity and triggers CASP3-dependent apoptosis [23]. These findings suggest that eIF6 may have been the initiator of cell death, but effector CASP3 inhibition prevents this effect, resulting in the continuous release of mitogen signals from cells and their eventual overproliferation. Nevertheless, more research is needed to fully understand the specific molecular pathways of eIF6 in a variety of biological activities.

According to the current study, the PI3K/AKT signaling pathway, cell cycle, and proteasomal degradation were among the eIF6-related signaling pathways that were activated in GC and may promote tumor invasion and proliferation. Through the suppression of apoptosis-related genes, including those encoding caspase-9, GSK-3, FoxO1 [24], Bcl-2-associated agonist of cell death (BAD), and Bcl-2 associated X (BAX), the PI3K/AKT signaling system is essential for cell preserve. The eIF signaling cascade is mostly regulated by the PI3K/AKT pathway since it is essential for regulating cell development and reproduction [25]. Furthermore, it has been established that eIF6 can enhance AKT- associated cancer pathway in a positive manner and support CRC's malignant tendencies [26].By using western blot, we were able to confirm that eIF6 positively controlled PI3K/AKT signaling by detecting the downregulation of phosphorylated PI3K/AKT (p-PI3K/AKT) after eIF6 expression was attenuated. This result was supported by the fact that overexpression of eIF6 positively correlated with invasive, proliferate, and cell cycle arrest of G0/G1, including cyclin A2 and CDK2, and negatively with the apoptotic marker Caspase 3, Cytochrome C, and PARP. This shows that the steady state eIF6 levels of expression in protein form were changed for various indicators. Stated differently, It's likely that the translational regulation of specific transcription elements by eIF6 controls their expression. Therefore, our findings provided a theoretical basis for eIF6-targeted GC treatment by indicating whether eIF6 promoted the cancerous development of GC via the PI3K/AKT signaling pathway.

Relevant research has demonstrated that the mTOR signaling pathway activates the eIF6 promoter in HCC cell lines, and that the FCN3 controls the transcription of eIF6 by binding ribosome maturation factor (SBDS) [27]. Nevertheless, our work did not examine the upstream regulatory mechanism involving eIF6, and more research on this mechanism is necessary. Furthermore, we ought to provide PI3K/AKT pathway stimulators or inhibitors to GC cells or animal models in order to identify the exact and comprehensive regulatory pathways that link eIF6 to PI3K/AKT-related signal molecules.

Conclusions

The study conclusively demonstrates that eIF6 is significantly overexpressed in gastric carcinoma (GC) and is intimately associated with advanced tumor progression and poorer patient outcomes. Our findings underscore the pivotal role of eIF6 in promoting cell proliferation and invasion, while concurrently suppressing apoptosis in GC. The direct linkage established between eIF6 and the PI3K/AKT signaling pathway, a well-known regulator of cell survival and growth, suggests that eIF6 could serve as a promising therapeutic target. Targeting eIF6 or its downstream effectors may open new avenues for GC treatment, potentially improving patient responses to therapy. The implications of this research are substantial, offering novel insights into GC pathogenesis and the potential for developing more effective treatment strategies.

Abbreviations

GC	Gastric Carcinoma
eIF6	Eukaryotic Translation Initiation Factor 6
PI3K/AKT	Phosphatidylinositol-4,5-Bisphosphate 3-Kinase/Protein Kinase B
TCGA	The Cancer Genome Atlas
GEO	Gene Expression Omnibus
IHC	Immunohistochemistry
ANOVA	Analysis of Variance
mRNA	Messenger Ribonucleic Acid
p-PI3K/AKT	Phosphorylated Phosphatidylinositol-4,5-Bisphosphate 3-Kinase/Protein Kinase B
WB	Western Blot

Supplementary Information

The online version contains supplementary material available at https://doi.org/10.1186/s12957-025-03746-w.

Additional file 1.

Additional file 2.

Additional file 3.

Acknowledgements

Not applicable.

Authors' contributions

SH conceived the idea of the study, performed the statistical analysis and collected tissue samples. HT participated in the experimental design and drafted and revised the article. ZKD scored and graded the immunohistochemical results. WCZ supervised the study and revised the article. All authors read and approved the final manuscript.All authors reviewed the manuscript.

Funding
This work was supported by the National Natural Science Foundation of China (82260555), Medical Innovation and Development Project of Lanzhou University(lzuyxex-2022–177), Major Science and Technology Projects of Gansu Province (22ZD6FA021-4), Joint Research Fund General Projects of Gansu Province (23JRRA1508), Gansu Provincial Top-notch Talent Program((2023) 9), Public Hospital High-quality Development of Scientific Research Project of Chinese Health Promotion Foundation (GL-C032) and Formulation process and lipid-regulating signaling pathway of hawthorn acidic constituents(2023YJA-10).

Data availability
No datasets were generated or analysed during the current study.

Declarations

Ethics approval and consent to participate
The study was approved by the Ethics Committee of The Medical Ethics Committee of Gansu Provincial People's Hospital. Lot No.2024-219. Signed written informed consent was obtained from the patients and/or their guardians.

Consent for publication
Not applicable.

Competing interests
The authors declare no competing interests.

Received: 23 October 2024 Accepted: 7 March 2025
Published online: 01 April 2025

References

1. Bray F, Laversanne M, Sung H, Ferlay J, Siegel RL, Soerjomataram I, Jemal A. Global cancer statistics 2022: GLOBOCAN estimates of incidence and mortality worldwide for 36 cancers in 185 countries. CA Cancer J Clin. 2024;74:229–63.
2. Wimmer B, Schernthaner J, Edobor G, Friedrich A, Poeltner K, Temaj G, Wimmer M, Kronsteiner E, Pichler M, Gercke H, et al. RiboScreen(TM) Technology Delivers a Ribosomal Target and a Small-Molecule Ligand for Ribosome Editing to Boost the Production Levels of Tropoelastin, the Monomeric Unit of Elastin. Int J Mol Sci. 2024;25:8430.
3. Arhab Y, Pestova TV, Hellen CUT. Translation of Overlapping Open Reading Frames Promoted by Type 2 IRESs in Avian Calicivirus Genomes. Viruses. 2024;16:1413.
4. Elliff J, Biswas A, Roshan P, Kuppa S, Patterson A, Mattice J, Chinnaraj M, Burd R, Walker SE, Pozzi N, et al. Dynamic states of eIF6 and SDS variants modulate interactions with uL14 of the 60S ribosomal subunit. Nucleic Acids Res. 2023;51:1803–22.
5. Brina D, Ponzoni A, Troiani M, Cali B, Pasquini E, Attanasio G, Mosole S, Mirenda M, D'Ambrosio M, Colucci M, et al. The Akt/mTOR and MNK/eIF4E pathways rewire the prostate cancer translatome to secrete HGF, SPP1 and BGN and recruit suppressive myeloid cells. Nat Cancer. 2023;4:1102–21.
6. Qi X, Zhang S, Chen Z, Wang L, Zhu W, Yin C, Fan J, Wu X, Wang J, Guo C. EGPI-1, a novel eIF4E/eIF4G interaction inhibitor, inhibits lung cancer cell growth and angiogenesis through Ras/MNK/ERK/eIF4E signaling pathway. Chem Biol Interact. 2022;352: 109773.
7. Zhao G, Zhang W, Dong P, Watari H, Guo Y, Pfeffer LM, Tigyi G, Yue J. EIF5A2 controls ovarian tumor growth and metastasis by promoting epithelial to mesenchymal transition via the TGFbeta pathway. Cell Biosci. 2021;11:70.
8. Alard A, Katsara O, Rios-Fuller T, Parra C, Ozerdem U, Ernlund A, Schneider RJ. Breast cancer cell mesenchymal transition and metastasis directed by DAP5/eIF3d-mediated selective mRNA translation. Cell Rep. 2023;42: 112646.
9. Herrmannova A, Jelinek J, Pospisilova K, Kerenyi F, Vomastek T, Watt K, Brabek J, Mohammad MP, Wagner S, Topisirovic I, Valasek LS. Perturbations in eIF3 subunit stoichiometry alter expression of ribosomal proteins and key components of the MAPK signaling pathways. Elife. 2024;13:RP95846.
10. Shaiken TE, Grimm SL, Siam M, Williams A, Rezaeian AH, Kraushaar D, Ricco E, Robertson MJ, Coarfa C, Jain A, et al. Transcriptome, proteome, and protein synthesis within the intracellular cytomatrix. iScience. 2023:26:105965.
11. Scagliola A, Miluzio A, Ventura G, Oliveto S, Cordiglieri C, Manfrini N, Cirino D, Ricciardi S, Valenti L, Baselli G, et al. Targeting of eIF6-driven translation induces a metabolic rewiring that reduces NAFLD and the consequent evolution to hepatocellular carcinoma. Nat Commun. 2021;12:4878.
12. Chih-Yang Wang DTMX P-HY, Chung-Yen Li,Gangga Anuraga,Hoang Dang Khoa Ta,Ming-Derg Lai,and Hui-Ping Hsu. Synergistic suppressive effects on triple-negative breast cancer by the combination of JTC-801 and sodium oxamate. Am J Cancer Res. 2023, 13:4661–4677.
13. Gao Y, Yuan L, Zeng J, Li F, Li X, Tan F, Liu X, Wan H, Kui X, Liu X, et al. eIF6 is potential diagnostic and prognostic biomarker that associated with (18) F-FDG PET/CT features and immune signatures in esophageal carcinoma. J Transl Med. 2022;20:303.
14. Gaikwad S, Ghobakhlou F, Young DJ, Visweswaraiah J, Zhang H, Hinnebusch AG. Reprogramming of translation in yeast cells impaired for ribosome recycling favors short, efficiently translated mRNAs. Elife. 2021;10:e64283.
15. Salaheldin YA, Mahmoud SSM, Ngowi EE, Gbordzor VA, Li T, Wu DD, Ji XY. Role of RONS and eIFs in Cancer Progression. Oxid Med Cell Longev. 2021;2021:5522054.
16. Pinzaglia M, Montaldo C, Polinari D, Simone M, La Teana A, Tripodi M, Mancone C, Londei P, Benelli D. EIF6 over-expression increases the motility and invasiveness of cancer cells by modulating the expression of a critical subset of membrane-bound proteins. BMC Cancer. 2015;15:131.
17. Sehrawat U. Exploiting Translation Machinery for Cancer Therapy: Translation Factors as Promising Targets. Int J Mol Sci. 2024;25:10835.
18. De Marco N, Tussellino M, Vitale A, Campanella C. Eukaryotic initiation factor 6 (eif6) overexpression affects eye development in Xenopus laevis. Differentiation. 2011;82:108–15.
19. Buzz Baum AS. On the origin of the nucleus- a hypothesis. Microbiol Mol Biol Rev. 2023;87: e0018621.
20. Sjovall D, Ghosh S, Fernandez-Fuentes N, Velasco-Hernandez T, Hogmalm A, Menendez P, Hansson J, Guibentif C, Jaako P. Defective ribosome assembly impairs leukemia progression in a murine model of acute myeloid leukemia. Cell Rep. 2024;43: 114864.
21. Jiang X, Li G, Zhu B, Yang J, Cui S, Jiang R, Wang B. p20BAP31 Induces Autophagy in Colorectal Cancer Cells by Promoting PERK-Mediated ER Stress. Int J Mol Sci. 2024;25:5101.
22. Clark AM, Magawa C, Pliego-Zamora A, Low P, Reynolds M, Ralph SJ. Tea tree oil extract causes mitochondrial superoxide production and apoptosis as an anticancer agent, promoting tumor infiltrating neutrophils cytotoxic for breast cancer to induce tumor regression. Biomed Pharmacother. 2021;140: 111790.
23. Challa S, Khulpateea BR, Nandu T, Camacho CV, Ryu KW, Chen H, Peng Y, Lea JS, Kraus WL. Ribosome ADP-ribosylation inhibits translation and maintains proteostasis in cancers. Cell. 2021;184(4531–4546): e4526.
24. Morgos DT, Stefani C, Miricescu D, Greabu M, Stanciu S, Nica S, Stanescu S II, Balan DG, Balcangiu-Stroescu AE, Coculescu EC, et al. Targeting PI3K/AKT/mTOR and MAPK Signaling Pathways in Gastric Cancer. Int J Mol Sci. 2024;25:1848.
25. Krassnig S, Leber SL, Orthmann A, Golob-Schwarzl N, Huber HJ, Wohlrab C, Skofler C, Pennauer M, Raicht A, Birkl-Toeglhofer AM, et al. Decreased eukaryotic initiation factors expression upon temozolomide treatment-potential novel implications for eIFs in glioma therapy. J Neurooncol. 2023;165:91–100.
26. Lin J, Yu X, Xie L, Wang P, Li T, Xiao Y, Zhou J, Peng S, Huang J, Luo Y, et al. eIF6 Promotes Colorectal Cancer Proliferation and Invasion by Regulating AKT-Related Signaling Pathways. J Biomed Nanotechnol. 2019;15:1556–67.
27. Ma D, Liu P, Wen J, Gu Y, Yang Z, Lan J, Fan H, Liu Z, Guo D. FCN3 inhibits the progression of hepatocellular carcinoma by suppressing SBDS-mediated blockade of the p53 pathway. Int J Biol Sci. 2023;19:362–76.

Publisher's Note